Charge Separation at Molecular Donor–Acceptor Interfaces: Correlation Between Morphology and Solar Cell Performance

Andreas Opitz, Julia Wagner, Wolfgang Brütting, Ingo Salzmann, Norbert Koch, Jochen Manara, Jens Pflaum, Alexander Hinderhofer, and Frank Schreiber

***Abstract*—Blends of organic electron and hole conductive materials are widely used for ambipolar charge-carrier transport and donor/acceptor (DA) photovoltaic cells. Thereby, the efficiency of these excitonic solar cells is correlated to the morphology of the interface between the donor and the acceptor materials, which in turns depends on the preparation conditions, the crystallization of the particular materials, and the interaction between the donor and acceptor molecules. In this contribution, the influence of the morphology on the solar cell architecture and performance will be discussed using different molecular DA combinations.**

***Index Terms*—Fullerene, interface morphology, organic heterojunctions, organic photovoltaic cells, perylene derivative.**

I. Introduction

In comparison to conventional (inorganic) semiconductor photovoltaic cells, the working mechanism of their organic counterparts differs in several fundamental aspects [1], [2]. The main difference can be found in the nature of the photoexcited states. In organic solar cells, the absorption of photons leads to the creation of strongly bound excitons instead of free electron–hole pairs [3]. Associated with high exciton-binding energies typically in the range between 0.2 and 1.5 eV in organic semiconducting materials [4], interfacial processes play a crucial role. To account for this characteristic property, the interface morphology of organic photovoltaic cells (OPVCs) has to be well controlled.

One reason for the high binding energy can be found in the comparatively low dielectric constant of organic materials resulting in a long range of the attractive Coulomb potential between an electron–hole pair. Furthermore, weak van der Waals interactions between individual molecules lead to a spatial restriction of the electronic wave function and thus a localization of electron–hole pairs in their mutual Coulomb potential well. Substantial progress toward an efficient charge-carrier separation, and with that toward efficient organic solar cells, was made in 1986 by Tang with the utilization of two organic materials with dissimilar electronic properties forming a donor–acceptor (DA) heterojunction [5]. Appropriate alignment of the energy levels of the donor and acceptor, respectively, enables successful exciton dissociation, which results in a geminate pair, i.e., a Coulombically bound hole polaron in the donor and electron polaron in the acceptor material.

For such a DA interface, charge generation can be split into a four-step process as illustrated in Fig. 1 [6].

1) Absorption of light and generation of excitons.
2) Exciton diffusion to the interface.
3) Exciton dissociation and charge-carrier generation at the interface.
4) Charge-carrier collection at the electrodes.

The overall charge generation process is quantified by the internal quantum efficiency [6]

$$\eta_{\rm int} = \eta_{\rm Abs}\eta_{\rm ED}\eta_{\rm CT}\,\eta_{\rm CC} \tag{1}$$

which is the product of the absorption efficiency $\eta_{\rm Abs}$, the exciton diffusion efficiency $\eta_{\rm ED}$, the charge-transfer efficiency $\eta_{\rm CT}$ and the charge-collection efficiency $\eta_{\rm CC}$. If reflection losses for coupling light from outside into the cell are taken into account, one obtains the external quantum efficiency $\eta_{\rm ext}$ that is basically the number of collected electrons with respect to the number of incident photons

$$\eta_{\rm ext} = (1-R)\,\eta_{\rm int} \tag{2}$$

with R being the reflectivity of the device.

$\eta_{\rm ext}$ is experimentally determined by the measured current density at short-circuit conditions ($J_{\rm SC}$) divided by the incident light intensity at a given wavelength. The overall power conversion efficiency η_P of a solar cell is given by

$$\eta_P = \frac{J_{\rm SC}V_{\rm OC}{\rm FF}}{P_{\rm in}} \tag{3}$$

where $V_{\rm OC}$ is the open-circuit voltage, FF is the fill factor, and $P_{\rm in}$ is the incident optical power density, preferably measured under AM1.5 sunlight conditions.

Manuscript received November 24, 2009; revised February 22, 2010; accepted March 28, 2010. Date of publication June 1, 2010; date of current version December 3, 2010. This work was supported by the German Research Foundation under the Priority Program 1355 ("Elementary Processes of Organic Photovoltaics").

A. Opitz, J. Wagner, and W. Brütting are with the Institute of Physics at the University of Augsburg, 86135 Augsburg, Germany (e-mail: Andreas.Opitz@physik.uni-augsburg.de; Wolfgang.Bruetting@physik.uni-augsburg.de).

I. Salzmann and N. Koch are with the Institute of Physics at the Humboldt University of Berlin, 10099 Berlin, Germany.

J. Manara is with the Bavarian Center for Applied Energy Research (ZAE Bayern), 97074 Würzburg, Germany.

J. Pflaum is with the Institute of Physics at the University of Würzburg, 97074 Würzburg, Germany, and also with the Center for Applied Energy Research (ZAE Bayern), 97074 Würzburg, Germany.

A. Hinderhofer and F. Schreiber are with the Institute of Applied Physics, University of Tübingen, 72076 Tübingen, Germany.

Color versions of one or more of the figures in this paper are available online at http://ieeexplore.ieee.org.

Digital Object Identifier 10.1109/JSTQE.2010.2048096

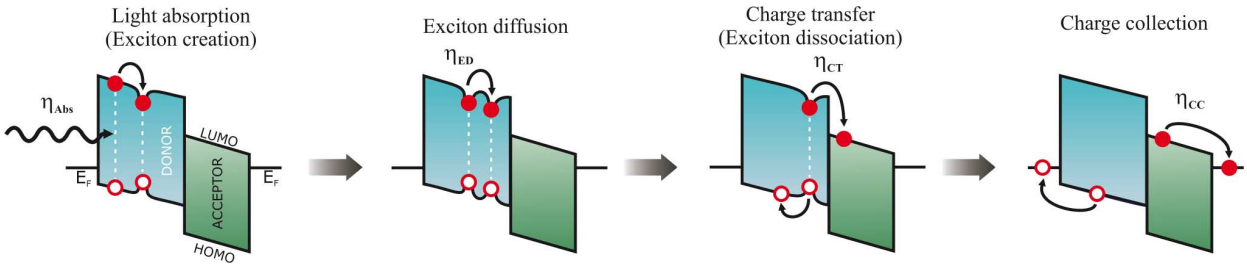

Fig. 1. Basic processes in organic solar cells related to the energy diagram of a DA cell. E_F are the Fermi energies of the cathode and anode contacts, respectively. LUMO is the lowest unoccupied molecular orbital, and HOMO is the highest occupied molecular orbital of the organic film. Filled circles represent electrons and open circles represent holes. A line between electron and hole symbolizes an exciton, while a dip in the energy levels depicts the lowering of energy by Coulomb interaction between electron and hole. η_{Abs}, η_{ED}, η_{CT}, and η_{CC} are the efficiencies of light absorption, exciton diffusion, charge transfer, and charge-carrier collection, respectively.

The typically high absorption coefficients of organic semiconductors ($\alpha \approx 10^5$ cm^{-1}) allow almost complete light absorption for sufficiently thick organic layers [7]. At suitable DA interfaces, the charge transfer is found to occur on time scales of a few hundred femtoseconds [8] yielding high charge-transfer efficiencies. Furthermore, also the charge-carrier collection efficiency in a planar heterojunction (PHJ) photovoltaic cell can be close to $\eta_{\mathrm{CC}} \approx 100\%$, if the charge-carrier mobility is sufficiently high [9]. However, one of the limiting factors is given by η_{ED}. The observed exciton diffusion lengths are typically a few nanometers only for molecular materials [7], [10], [11], which is significantly shorter than the optical absorption length (100–200 nm) required for absorbing a significant fraction of the incident light [6]. To overcome this exciton diffusion bottleneck, different strategies to increase the active volume of the cell have been employed with the bulk heterojunction (BHJ) and the multiheterojunction approach being probably the most successful ones [7], [9], [12]–[14]. Using these concepts, it has been demonstrated that power conversion efficiencies exceeding 5% can be achieved both with polymers and tandem cells using molecular materials [15]–[17].

Numerous studies on conjugated polymer/methanofullerene blends have shown that mixing donor and acceptor materials in a BHJ cell, though being very simple in principle, can lead to significant variations in cell performance, mostly due to different film morphologies [18]. It was found that in blends of a poly(phenylenevinylene) derivative (MDMO-PPV) and the soluble fullerene derivative phenyl-C61-butyric acid methyl ester (PCBM) with a PCBM content exceeding 67 wt% a molecular dispersion with 1:1 stoichiometry is superimposed by a large-scale interpenetrating network with pronounced percolation pathways. Recent numerical simulations show that not only the length scale of the phase separation between donor and acceptor but also the orientation of the phase-separated regions with respect to the electrodes plays a crucial role [19]. It turns out that phase-separated nanopillars with diameters in the range of the exciton diffusion length and growth direction perpendicular to the electrodes are most favorable for achieving low recombination losses accompanied by high charge-carrier mobilities to achieve efficient charge collection.

For OPVCs based on small-molecule materials, which are the focus of this study, there are different possible device structures under consideration: a BHJ-fabricated by coevaporation of donor and acceptor molecules [20] and the planar (multi)heterojunction obtained by sequential evaporation of both materials [7], [21]. A further improvement of device performance could be realized by a hybrid DA heterostructure, i.e., a blend sandwiched between neat donor and acceptor layers, providing efficient exciton dissociation and simultaneously maintaining good charge-carrier transport toward the electrodes [22]. In spite of the huge amount of work related to the growth of a single molecular material on various kinds of substrates, there are very little systematic growth studies on molecular blends till date. Particularly, there is a lack of investigations of the correlation between film morphology under controlled growth conditions and microscopic processes in the corresponding solar cell. Furthermore, the number of materials for which these studies have been performed is quite limited, comprising basically only Cu- or Zn-phthalocyanine combined with the Buckminster fullerene (C_{60}) or perylene derivatives [e.g., (3,4,9,10-perylenetetracarboxylic-bis-benzimidazole (PTCBI)]. Bilayers and blends of copper phthalocyanine (CuPc) and C_{60} were investigated as a function of deposition conditions and layer composition [23]. An enhancement of OPV power conversion efficiency by a factor of two was obtained in going from a PHJ via fully mixed blends to a structure with a compositional gradient from the pure donor material at the anode to the pure acceptor at the cathode [24]. It was shown that the morphology of CuPc:PTCBI blends can be altered by postdeposition annealing, if covered with a metal electrode [9]. Furthermore, the morphologies and device performance of CuPc:C_{60} mixtures grown by standard thermal evaporation and vapor phase deposition using gas flow were compared [25].

II. Materials and Solar Cell Architectures

The focus of our joint studies is to address the correlation between film and interface morphology and the photoelectrical properties of molecular DA cells. Fig. 2 shows different possible architectures, where an interface for exciton dissociation is present. The simplest case is a well-defined sharp interface [see Fig. 2(a)] between the donor and the acceptor layer (PHJ). By creating a roughened or an interdigitated layer structure [see Fig. 2(b) and (c)], the effective interfacial area can be increased. In a BHJ, the DA interface is distributed over the entire blended film either as a homogenous molecular mixture,

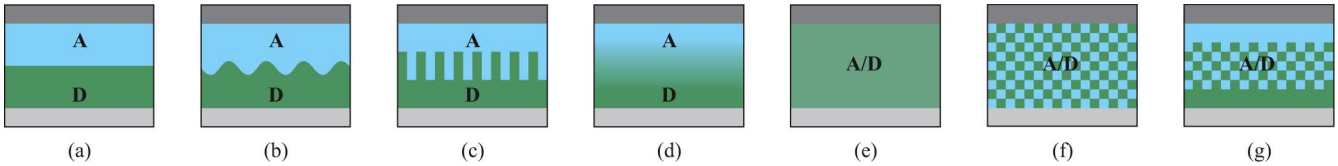

Fig. 2. Different architectures for solar cells. (a) PHJ. (b) DA heterojunction with rough interface. (c) Planar DA layers combined with interdigitated interface. (d) Gradient heterojunction. (e) BHJ (molecular mixture). (f) Phase-separated BHJ. (g) PHJ with mixed interface.

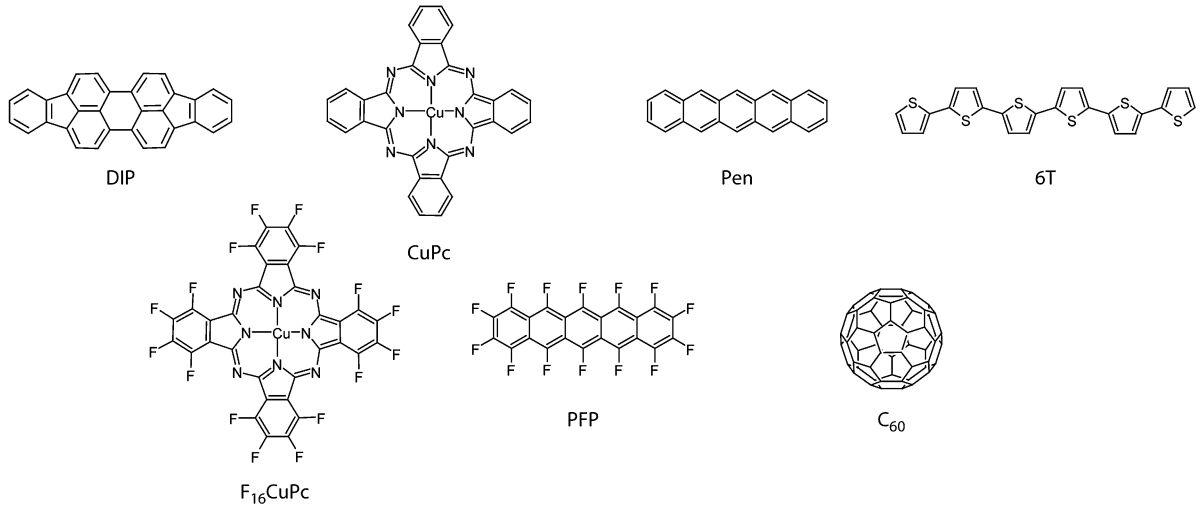

Fig. 3. Chemical structures of the molecular donor materials (DIP: diindenoperylene; CuPc: copper phthalocyanine; Pen: pentacene; 6T: sexithiophene) and the molecular acceptor materials (F_{16}CuPc: perfluorinated CuPc; PFP: perfluorinated Pen; C_{60}: Buckminster fullerene).

a compositional gradient or as a (nano)phase-separated system [see Fig. 2(d)–(f)]. The length scale of the phase separation can be influenced by postdeposition annealing in polymer [26] and molecular [9] solar cells. Such a distributed interface allows for exciton dissociation, even if the exciton diffusion length is rather low. Furthermore, the realization of percolation pathways for unhindered transport of charge carriers to the electrodes is important. However, for optimizing the overall efficiency of a photovoltaic device, it has to be taken into account that the efficiencies of the individual processes are partly connected to each other. An additional structure providing an increased DA interface in the active layer and simultaneously accounting for an efficient transport of both charge carriers to the electrodes is a PHJ with a diffuse interface, the so-called planar-mixed heterojunction (PM-HJ) [see Fig. 2(g)]. The neat transport layers underneath and on top of the mixed photoactive layer prevent shortcuts between the electrodes by pathways of one material in the blend and reduce damage of the photoactive layer by deposition of the top metal contact.

It is not to be expected that all these different interface morphologies can be realized with one single DA combination. We have, therefore, looked at several donor and acceptor materials shown in Fig. 3 and have fabricated both PHJ and BHJ devices from different combinations of them. The chosen materials are CuPc, pentacene (Pen), diindenoperylene (DIP), and sexithiophene (6T) as donor together with Buckminster fullerene (C_{60}), perfluorinated CuPc (F_{16}CuPc), and perfluorinated Pen (PFP) as acceptor. The motivation behind the choice of materials was that depending on the shape of the different molecular species, being

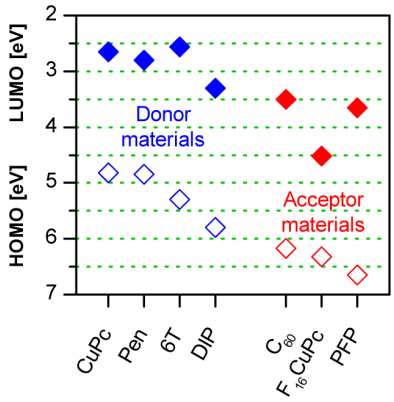

Fig. 4. Energy levels of the HOMO (filled symbols) and the LUMO (open symbols) for the investigated materials. The values are taken from the literature [4] and [28]–[30] and indicate the energy levels of the respective charge carriers. The LUMO for DIP is calculated from the HOMO [30] and the relation of the optical gap and the transport gap in reference [4]. The materials are sorted with decreasing value of the HOMO level.

spherical such as C_{60}, disk-shaped like the CuPc's or rod-like as 6T, DIP, Pen, and PFP, one could expect to observe different film growth scenarios, in particular in BHJ structures. Additionally, as indicated in Fig. 4, the materials cover a wide range of energy levels of their highest occupied molecular orbital (HOMO) and their lowest unoccupied molecular orbital (LUMO). Assuming vacuum-level alignment at the DA interface, an upper limit for the achievable open-circuit voltage (V_{OC}) can be estimated from the intermolecular gap, the difference between the HOMO of the donor and the LUMO of the acceptor. (Interface dipoles as

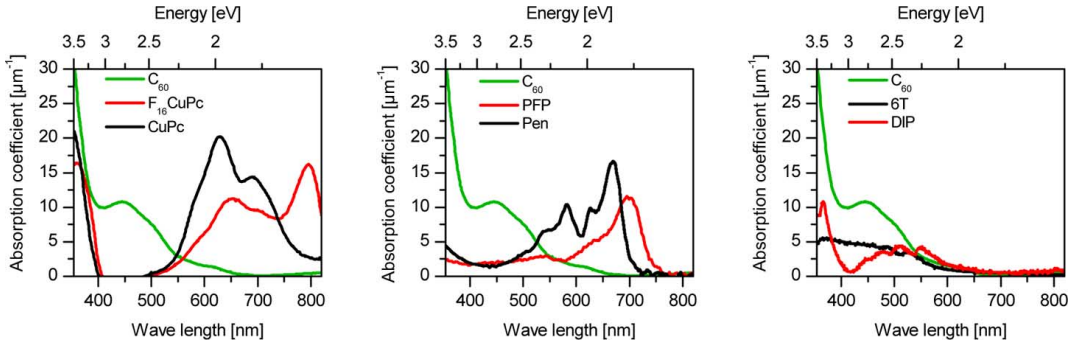

Fig. 5. Absorption spectra of the investigated materials. The spectra are calculated from transmission measurements on transparent substrates.

reported for the CuPc/C_{60} interface [27] are neglected in the estimation.)

A third issue to be considered is the different strength and spectral range of light absorption. Fig. 5 shows absorption spectra of the used materials calculated from transmission measurements on transparent substrates. In order to increase the short-circuit current (J_{SC}), harvesting a large portion of the solar spectrum is important, which is particularly challenging for the red and near-infrared spectral regions. To meet this requirement, the absorption spectra of donor and acceptor materials should preferably complement one another as it is the case for the donor materials CuPc or Pen combined with the acceptor C_{60}. All other DA combinations show relatively large spectral overlap and thus provide less favorable conditions for high degrees of absorption over the entire solar spectrum. Furthermore, the maximum absorption coefficient in the visible part of the spectrum differs considerably among the chosen materials. This is partly due to different oscillator strengths of the involved electronic transitions, but partly a consequence of the optical anisotropy of the materials. Especially for 6T and DIP, the direction of the transition dipole moment is along the long molecular axis, which has for the consequence that films with preferentially upright standing molecules are only relatively weakly absorbing optically [31]. In contrast, Pen shows higher absorption in spite of standing molecules because the transition dipole moment is along the short molecular axis in this case [32].

The aim of this paper is to give an overview of our ongoing study on the comparison of different solar cell architectures realized by the aforementioned material combinations. We will focus on three particular systems, namely CuPc and C_{60}, Pen with C_{60} and the combination of CuPc and its perfluorinated analogue F_{16}CuPc, as they exhibit three different prototypes of phase formation behavior in a BHJ mixture. For details on device fabrication, measurement conditions, and an in-depth discussion of the results, we refer to [33] and [34]. At the end, we will present some new results on 6T/C_{60} and DIP/C_{60} devices showing very promising performance as PHJs, but certainly need further investigation and optimization.

III. Interface Morphology and Solar Cell Performance

The results described in the following were obtained on films grown by molecular beam deposition in high vacuum. As substrate, indium tin oxide (ITO) glass precoated with a thin layer (∼25 nm) of the conducting polymer poly(3,4-ethylenedioxythiophene) poly(styrenesulfonate) (PEDOT:PSS) was used. Film growth was performed either with the substrate kept at room temperature or at about $100\,^{\circ}$C (as indicated in the respective figure captions). For device characterization, an exciton blocking layer (as mentioned in the figure caption) and a counter electrode (LiF/Al, Al, or Sm) were applied by thermal evaporation in a crossbar architecture, yielding active device areas of about $4\ \mathrm{mm}^2$. Morphological characterization was performed using a scanning force microscope (SFM) under ambient conditions, while photoelectrical measurements were conducted in a nitrogen filled glove box or in a vacuum chamber. The light intensities of the simulated AM1.5 sun spectrum have been measured with a $1 \times 1\ \mathrm{cm}^2$ calibrated reference cell (LOT-Oriel, calibrated against NREL standard). Nevertheless, as the perfect homogeneity of the light beam cannot be guaranteed, the power conversion efficiency of cells with smaller sizes might be overestimated. No corrections accounting for spectral mismatch have been performed [35].

We would also like to note that the device performance shows some variations from sample to sample, depending on the detailed device fabrication conditions (e.g., thickness control, substrate temperature, and evaporation rates). To account for this, all different device types have been repeatedly fabricated and characterized. The numbers reported later on in Table I indicate the spreading of the obtained device parameters. It is also important to mention that the type of metal used for the top contact and the usage of an exciton blocking interlayer have been independently tested and optimized for each DA combination. Hence, the device structures reported here are not necessarily identical for the different material systems. However, within a given DA combination, we always compare planar and BHJ devices with the same stack design so that conclusions about the influence of the DA interface morphology are not severely affected by the choice of the contacts or by the presence of an exciton blocker.

A. *CuPc–C_{60}*

The combination of CuPc and C_{60} is a well-known molecular DA combination with favorable conditions for light harvesting due to their complementary absorption spectra and high absorption coefficient over almost the full visible range [36]. As the absorption of the phthalocyanine (see Fig. 5) and the acceptor

TABLE I
COLLECTION OF THE DETERMINED POWER CONVERSION EFFICIENCIES, OPEN-CIRCUIT VOLTAGES, FILL FACTORS, AND SHORT-CIRCUIT CURRENT DENSITIES OF THE INVESTIGATED SOLAR CELLS

Solar cell			η [%]	V_{OC} [V]	FF [%]	J_{SC} [mA/cm^2]
CuPc/C_{60}	PHJ	(without blocking layer)	$0.2-0.7$	$0.50-0.53$	$26-32$	$1.2-4.0$
CuPc:C_{60}	BHJ	(without blocking layer)	$0.3-0.9$	$0.35-0.46$	$31-37$	$4.1-6.8$
CuPc:C_{60}	PHJ	(with blocking layer)	$1.3-2.3$	$0.50-0.56$	$34-55$	$5.5-7.7$
CuPc:C_{60}	PM-HJ	(with blocking layer)	$0.9-1.8$	$0.48-0.55$	$22-33$	$7.4-10.6$
CuPc/F_{16}CuPc	PHJ			no photocurrent		
CuPc:F_{16}CuPc	BHJ		<0.01	0.36	23	0.012
DIP/C_{60}	PHJ		$2.8-3.9$	$0.88-0.94$	$60-74$	$4.6-5.4$
6T/C_{60}	PHJ		$1.0-1.6$	$0.41-0.49$	$39-59$	$5.0-10.5$
Pen/C_{60}	PHJ[a]		—	$0.22-0.25$	$28-33$	$1.4-2.8$
Pen:C_{60}	PM-HJ[a]		—	$0.28-0.29$	$26-31$	$0.7-0.9$

[a]Noncalibrated light source.
The given ranges indicate the spreading of the obtained device parameters for samples prepared under comparable preparation conditions. Except for Pen/C_{60}, the illumination was simulated AM1.5 sunlight conditions with 100 mW/cm^2.

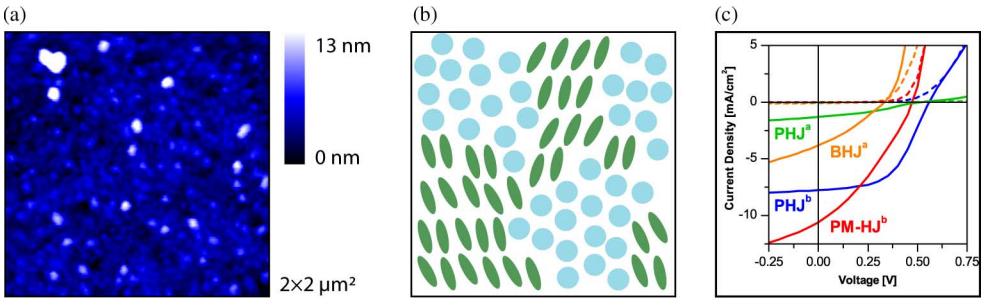

Fig. 6. Analysis of the CuPc–C_{60} material combination. (a) Scanning force microscopy image of a 1:1 mixture. (b) Cartoon of the morphology in this phase-separated blend. (c) Current–voltage characteristics of the PHJ and the BHJ (superscript a: both without an exciton blocking layer) as well as the PHJ and the PM-HJ (superscript b: both with an exciton blocking layer) in the dark and under 100 mW/cm^2 simulated AM1.5 illumination. The layer structure for the PHJ^a is ITO/PEDOT:PSS/CuPc (40 nm)/C_{60} (40 nm)/LiF/Al, for the BHJ^a ITO/PEDOT:PSS/CuPc:C_{60} = 1:1 (80 nm)/LiF/Al, for the PHJ^b ITO/PEDOT:PSS/CuPc (40 nm)/C_{60} (60 nm)/BCP (8 nm)/Al, and for the PM-HJ^b ITO/PEDOT:PSS/CuPc (3.5 nm)/CuPc:C_{60} = 1:1 (50 nm)/C_{60} (5 nm)/BCP (8 nm)/Al.

strength of the fullerene [37] are high, this material combination became a model system for analyzing molecular solar cells. An external quantum efficiency of 5.0% was achieved with this system [22] in a BHJ device with adjacent neat transport layers. It was shown furthermore that by variation of the annealing temperature, the microstructure can be modified to improve the solar cell efficiency [9].

Neat films of CuPc and C_{60} grow as relatively smooth layers exhibiting a polycrystalline morphology with typically needle-like crystallites for CuPc and more spherical grains for C_{60} [33]. However, if both materials are coevaporated to form a blend, a markedly different film morphology is obtained due to the dissimilar molecular shape. Fig. 6(a) shows an SFM image of a 1:1 blend with considerable roughness and island structures [38], [39]. Although, the exact phase composition of these features remains to be determined, a plausible explanation of this morphological observation is given by a phase separation, resulting in nanoscaled grains of each material. Fig. 6(b) displays a simplified schematic of the suggested morphology inside these blends, assuming that both materials are not miscible. Recently, evidence for phase separation in CuPc:C_{60} blends was reported from X-ray scattering [33]. The mixed film shows the same Bragg peak positions as layers of the neat materials corresponding to the α-phase of CuPc and the fcc-structure of C_{60}. This fact can be traced back to the simultaneous existence of CuPc and C_{60} crystallites in the blend. Nevertheless, we would like to mention that also featureless SFM images for these mixtures have been reported in the literature [24], reflecting probably slightly different film growth conditions in different laboratories.

Charge-transport properties of mixed films have earlier been investigated in FETs [40], [41] and photodiodes [33], [42]. Both electron and hole mobilities were found to decrease exponentially in blends with decreasing content of the electrically conducting molecular species. This is in full agreement with the picture of nanophase separation resulting in charge-carrier transport by percolation through the respective pathways of each species.

The performance of this material combination has been studied in photovoltaic cells utilizing either a PHJ or a BHJ (1:1 blend). Typical current–voltage characteristics in the dark and under simulated AM1.5 conditions are depicted in Fig. 6(c) and the photovoltaic parameters are given in Table I. Furthermore the characteristics of a PHJ and a PM-HJ with an exciton blocking layer of bathocuproine (BCP) are shown. As general observation, we find in cells with mixed layers (BHJ and PM-HJ) higher short circuit currents J_{SC} in comparison to the respective planar heterojunctions, indicating more efficient exciton dissociation

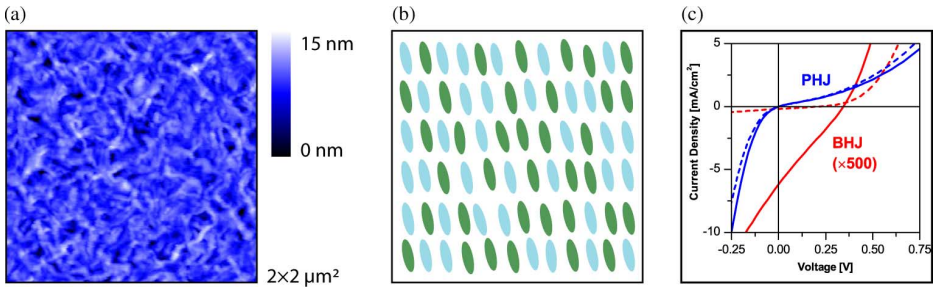

Fig. 7. Analysis of the CuPc–F_{16}CuPc material combination. (a) SFM image of a 1:1 mixture evaporated at 100 °C substrate temperature. (b) Cartoon of the morphology in this molecularly mixed blend. (c) Current–voltage characteristics of the PHJ and the BHJ in the dark and under 100 mW/cm^2 simulated AM1.5 illumination. The layer structure for the PHJ is ITO/PEDOT:PSS/CuPc (40 nm)/F_{16}CuPc (40 nm)/LiF (0.5 nm)/Al and for the BHJ ITO/PEDOT:PSS/CuPc:F_{16}CuPc = 1:1 (80 nm)/LiF (0.5 nm)/Al.

due to an increased interfacial area [33], [42]. Unfortunately, this benefit is accompanied by a decrease in the open-circuit voltage V_{OC}, e.g., from 0.56 V for the PHJ cell to 0.49 V for the PM-HJ cell. V_{OC} is mainly defined by the intermolecular gap between the LUMO of the acceptor and the HOMO of the donor. Earlier studies of this material combination showed a reduced intermolecular gap in blended films [42], [43]. Additionally, coupling of the quasi-Fermi levels in the blend to the electrode materials is different for the bulk and PHJs [44]. The low FF in the PM-HJ may partly be assigned to inappropriate layer thicknesses and subsequently high series resistance [24]. Also, for other molecular materials, it was shown that the FF in solar cells containing blended films is lower than in PHJ cells [45]. The layer thickness of the organic blend might exceed the thickness in which percolation pathways reach the electrodes from the whole volume of the device. The current–voltage characteristics of the PHJ device without an exciton blocking layer is affected by an S-shape behavior, i.e., a low current density near and above V_{OC}, which reduces FF. The appearance of this undesired feature has recently gained more and more attention in the literature. Uhrich *et al.* could relate the S-shaped current–voltage characteristics to insufficient energy level alignment between the photoactive layer system and the hole transport layer of a PHJ device. An accumulation of charge carriers inside the device leads to suppressed forward current as well as reduced photocurrent in the vicinity of V_{OC} [44]. A similar explanation of the "kink" in the current–voltage curve close to V_{OC} was given by Nelson *et al.* Based on a simple model of a molecular photovoltaic device as a two-level light absorbing system, the S-shaped characteristic was connected to slow charge transfer originating from large energy steps at the electrodes [46]. Furthermore, degradation studies on Pen/C_{60} heterojunction solar cells related the deterioration of device performance, manifested in a continuous decrease of FF, with photooxidation and UV annealing [47]. The effect is explained by the reorganization of Pen near the ITO substrate resulting in an ITO/Pen interface barrier. The responsibility of interfaces for the S-shaped characteristics is also confirmed by Kumar *et al.* [48] and Glatthaar *et al.* [49], ascribing this anomalous feature to a charge-extraction barrier as a result of interfacial dipoles [48] and a hindered charge transfer at one of the electrical contacts caused by the corrosion of the contact metal, respectively.

Compared to the similarly structured solar cells based on CuPc/C_{60} [50], our OPVCs show lower power conversion efficiencies, although an exciton blocking layer BCP is used that prohibits quenching of excitons at the electrode [51]–[54]. The reason may be found in nonoptimized layer thicknesses. Optimization of this parameter is indispensable for high efficiencies of exciton diffusion and charge-carrier collection and to exploit optical interference effects inside the device [36]. Nevertheless, a free variation of the film thicknesses is partially limited as the rough morphology of the organic layers requires sufficiently thick films to avoid undesirable leakage in the current–voltage measurement.

B. *CuPc–F_{16}CuPc*

Fluorination of organic molecules is a well-known method to tune the electrochemical potentials of a material toward higher electron affinity and ionization potential, leaving the energy gap of the phthalocyanines more or less unaffected [55], [56]. In this way, a donor-type material (such as CuPc) can be turned into an electron acceptor. We have, therefore, studied bilayers and blends of the H-terminated (H_{16}-)CuPc with its fully fluorinated analogue F_{16}CuPc. In contrast to the aforementioned system, both materials are structurally very similar (disk shape) so that a completely different film growth scenario and phase behavior could be expected in their mixtures.

Blends of CuPc:F_{16}CuPc show the same SFM morphology as the neat films of CuPc and F_{16}CuPc (see Fig. 7(a) and [57]). Due to similar size and shape of both molecules and very similar packing motifs in neat crystalline films of each material, they are able to form a molecularly mixed crystalline structure [57]. Thereby, the lattice spacing of the blend is in between the values for the neat films. A similar scenario was observed for Pen/PFP [58] and other rod-like molecules [59], such as 6T, sexiphenyl and dihexylsexithiophene. A schematic sketch illustrating the morphological concept of a molecularly mixed phthalocyanine film is presented in Fig. 7(b). This molecular packing characterized by an alloy of two materials with different energy levels in alternating DA stacks leads to an electrical transport behavior markedly different to that of phase-separated blends. We find that unipolar electron and hole transport is possible in these molecularly mixed films; however, if both carrier types are injected at the same time (or are photogenerated

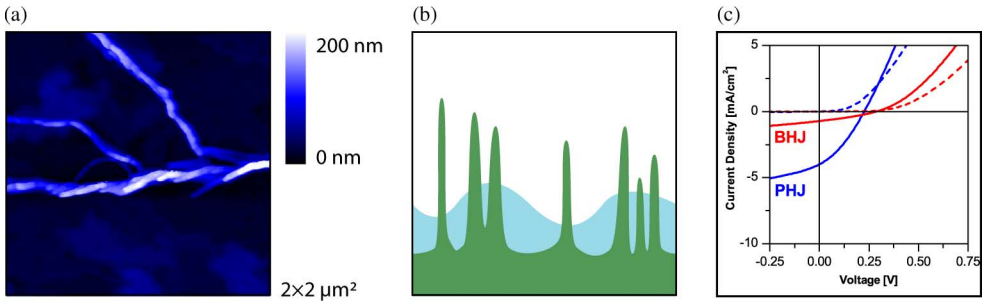

Fig. 8. Analysis of the Pen–C_{60} material combination. (a) SFM image of a 1:1 mixture. (b) Cartoon of the morphology with a large-scale phase separation (different scale as in Figs. 6 and 7). (c) Current–voltage characteristics of the PHJ and the PM-HJ in the dark and under halogen lamp illumination. The layer structure for the PHJ is ITO/PEDOT:PSS/Pen (50 nm)/C_{60} (50 nm)/Sm and for the PM-HJ ITO/PEDOT:PSS/Pen (5 nm)/Pen:C_{60} = 1:1 (60 nm)/C_{60} (5 nm)/Sm.

by light absorption), the current decreases by several orders of magnitude [57]. A conclusive explanation can be found in the formation of charge-transfer states with a hole located at the CuPc molecule and an electron sitting on the neighboring F_{16}CuPc molecule. Such a charge-transfer state is unaffected by the electric field and the involved molecules are subsequently blocked for a further charge-carrier transport.

This behavior leads to very low photocurrents in the BHJ solar cell as shown by the current–voltage characteristics in Fig. 7(c). Also included in this figure are the J–V characteristics for a PHJ device of both materials. Interestingly, for this device, the current under reverse-biasing is much higher than under forward-bias conditions. This is related to the formation of a charge-generation layer at the DA interface, where charge-carrier pairs are generated by tunnelling of electrons from the HOMO of CuPc into the LUMO of F_{16}CuPc [60]. However, for the PHJ, there is almost no effect of illumination as manifested in a negligible value of V_{OC}.

The overall performance of this material combination in photovoltaic cells is very poor. Apart from the small open-circuit voltage (which was to be expected already from the energy level diagram in Fig. 4), the extremely low photocurrents in blends make them useless as active layer in OPV applications. The general lessons to be learned is that this type of mixed crystalline films of donor and acceptor molecules is not desirable for efficient OPV cells, as it prevents charge-carrier separation (the same scenario is by the way found in Pen/PFP [58]).

C. Pen–C_{60}

Pen is one of the most intensively studied organic semiconductor materials, mainly due to its high charge-carrier mobilities observed in organic FETs [61]. However, in the context of OPV devices, there is comparatively little study reported in the literature on PHJs [47], [62], [63], although from the viewpoint of optical absorption, the combination with C_{60} should be quite promising.

The surface morphology of coevaporated Pen:C_{60} films deposited on the top of a Pen precoverage determined by SFM is depicted in Fig. 8(a). Together with X-ray scattering, it was shown that, similar to the CuPc/C_{60} system, phase separation takes place [34]; however, in contrast to the former system, the length scale is much larger in this case due to the strong crystallization tendency of Pen. A schematic of the resulting morphology with Pen crystallites extending beyond the C_{60} layer is shown in Fig. 8(b). A detailed analysis of the mobility is pending, but due to the large-scale phase separation, no strong influence on the charge-carrier transport is expected as compared to neat films.

The characteristics of the PHJ and PM-HJ solar cells are shown in Fig. 8(c). In contrast to the CuPc/C_{60} system, the behavior of J_{SC} and V_{OC} is different in planar and BHJs. Here, the PM-HJ has the higher open-circuit voltage, but a lower short-circuit current. However, it seems to be obvious that large-scale phase separation and the formation of large Pen crystals are not favorable for solar cell performance. The observed Pen needles extending through the C_{60} layer can lead to leakage. Additionally, the distance between the needle-like Pen islands is on the length scale of micrometers and thus far too big in comparison to the observed exciton diffusion length in C_{60}, which further limits efficient exciton dissociation.

D. DIP/C_{60} and 6T/C_{60}

Besides the widely spread and intensively studied materials CuPc and Pen, we have recently started investigations on two rather uncommon molecular donor materials: 6T and DIP. Both the materials have been used in combination with C_{60} as acceptor. Structural formulas, energy levels, and absorption spectra are depicted in Figs. 3–5. Detailed studies on structure, morphology, charge-carrier mobility, and especially their correlation with solar cell performance are currently under study. Absorption coefficients are comparatively low in both materials (see Fig. 5), which can be attributed to predominantly upright standing molecules proven by X-ray scattering measurements and predicted by various structural investigations [64]–[66]. Although, this leads to an unfavorable orientation of the optical transition dipole regarding the absorption of incoming light, we have observed remarkably high power conversion efficiencies already in simple PHJs. We, therefore, expect that these materials could hold further potential for efficient solar cells.

Up to now, DIP has not yet been investigated in organic solar cells. Recently, a similarly constructed molecule tetraphenyldibenzoperiflanthene (DBP) was used in PHJ organic solar cells exhibiting power conversion efficiencies of up to 3.6% [67]. The high V_{OC} and J_{SC} of the DBP-based cell

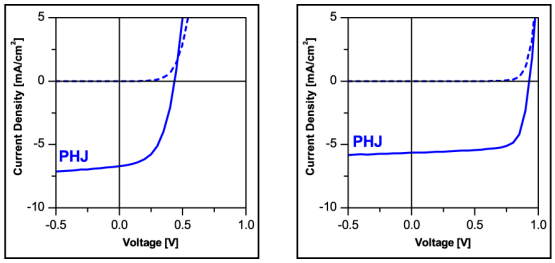

Fig. 9. Device characteristics for 6T/C_{60} and DIP/C_{60} PHJ solar cells in the dark and under 100 mW/cm^2 simulated AM1.5 illumination. The layer structure for the PHJs are ITO/PEDOT:PSS/6T (50 nm)/C_{60} (60 nm)/Al and ITO/PEDOT:PSS/DIP (50 nm)/C_{60} (80 nm)/BCP (8 nm)/Al, respectively. The DIP layer was evaporated at 100 °C substrate temperature.

is attributed to its high HOMO level and the effective light absorption, respectively. The latter argument cannot be applied in the case of DIP, which shows quite low absorption coefficient, at least compared to CuPc and Pen, and has strong spectral overlap with C_{60}. Furthermore, DIP has been shown to have balanced charge-carrier transport along the c' direction in single crystals [68] and remarkably high exciton diffusion lengths of $\approx$100 nm [69]. Even though the absolute values are actually discussed in the literature [7], [10], [11], and [69], a correlation between structural coherence length and exciton diffusion length is reasonable, meaning that better film crystallinity should give rise to higher exciton diffusion length [70]. A detailed study of DIP film growth on OPV relevant substrates, the resulting morphology, and its relation to device performance is currently under way and will be reported elsewhere [71].

The theoretical maximum value of V_{OC} is a function of the difference between HOMO of the donor and LUMO of the acceptor, minus the binding energy of the dissociated, geminate electron–hole pair [72]. Thus, from the compilation of the molecular energy levels in Fig. 4, we expect a high V_{OC} for the combination of DIP with C_{60}, which was approved by current–voltage characteristics (see Fig. 9). Together with a nearly rectangular shape of the J–V curve, resulting in a high FF reaching up to 74%, power conversion efficiencies of 3.9% under 100 mW/cm^2 illumination were achieved. The photovoltaic parameters are given in Table I to compare the different material combinations.

6T has been used as donor material in BHJ solar cells already in 1997 [73], where blends of 6T and C_{60} exhibited microphase-separated morphology, as revealed by transmission electron microscopy studies. More efficient BHJ solar cells of the same material combination have been reported recently by Alem *et al.*, reaching $\eta = 1\%$ after reverse bias annealing [74]. As in the case of DIP, 6T molecules are standing upright on the substrate and thus have rather low absorption coefficients as well as a large spectral overlap with the absorption spectrum of C_{60}, both providing *a priori* unfavorable conditions for efficient light harvesting.

As was expected from energy level alignment, V_{OC} of 6T/C_{60} PHJ solar cells is lower than for DIP/C_{60} cells (see Fig. 9). Nevertheless, relatively high short-circuit current densities and high FFs lead to efficiencies of up to 1.5%. Reasonable photocurrents have also been observed in PHJ cells with thick 6T layers (400–500 nm), which indicate that the exciton diffusion length might be considerably larger as compared to that of CuPc. So, there is room for significant further improvement by either controlling the molecular orientation or by a systematic layer thickness variation, thereby matching light absorption, exciton diffusion, and charge-carrier extraction lengths.

IV. Summary and Outlook

In this contribution, we give an overview of our study on growth and photovoltaic characterization of different molecular DA systems. Apart from PHJs, which have been fabricated for all DA combinations, we have particularly looked at the phase behavior and the resulting morphology of BHJs between selected materials. Owing to the differences in molecular shape, we have been able to prepare and identify three different growth scenarios leading to largely different interface morphologies and observed their consequences for device performance. Blends of CuPc and C_{60} show nanophase separation on a length-scale of a few ten nanometers, being spatially separated not too far from the expected exciton diffusion range. Additionally, this system shows very favorable spectral properties for light harvesting over the whole visible range. However, we also have seen limitations in the transport properties of this material system leading to low FFs and S-shaped J–V characteristics, in particular, in PHJ devices. The combination of CuPc with its perfluorinated analogue F_{16}CuPc leads to the formation of a molecularly mixed "organic alloy". However, such an intimate mixing is not favorable for charge separation in photovoltaic cells as the primarily formed charge-transfer states are Coulombically bound. The mixing behavior of Pen/C_{60} represents the other extreme case exhibiting phase separation on a very large length scale (larger than the nominal layer thickness). In addition to the obvious mismatch of the resulting interface morphology with the exciton diffusion length, these large Pen crystallites lead to undesired leakage pathways for charge carriers.

Apart from these classical material systems, we have recently started investigating PHJs of DIP and 6T with the acceptor C_{60}. These donor materials are well known to form highly ordered thin films with excellent charge-transport properties. However, due to their tendency to grow in a fashion, where the molecules are standing almost upright on the substrate and the fact that the transition dipole moment is oriented along the long axis of the molecule, their optical absorption is by far weaker than, for example, in CuPc and Pen. Nevertheless, first results are very promising already in PHJ devices with nonoptimized layer thicknesses. In particular, DIP/C_{60} with an open-circuit voltage of 0.9 V and a FF of more than 70% has the potential for high-efficiency photovoltaic cells.

To conclude, the route toward high-efficiency molecular solar cells still holds many challenges. Phase behavior and morphology formation in molecular blends is still not very well understood, and it is obvious that the vision of tailoring interface morphologies, as indicated in Fig. 2, is not straightforward

and for sure not possible with one single material combination only. Besides molecular self-assembly and thermodynamically driven phase separation followed so far, there are currently increasing efforts to create artificial phase separation following the scenarios sketched in Fig. 2(b) and (c) by glancing angle deposition [75] or by stamping techniques [76], [77]. Additionally, the search for well-ordered materials with better charge and exciton transport properties could be a viable alternative to the BHJ concept.

REFERENCES

[1] C. J. Brabec, V. Dyakonov, J. Parisi, and N. S. Sariciftci, *Organic Photovoltaics*. Berlin, Germany: Springer-Verlag, 2003.

[2] B. A. Gregg and M. C. Hanna, "Comparing organic to inorganic photovoltaic cells: Theory, experiment, and simulation," *J. Appl. Phys.*, vol. 93, pp. 3605–3614, 2003.

[3] B. A. Gregg, "The photoconversion mechanism of excitonic solar cells," *MRS Bull.*, vol. 30, pp. 20–22, 2005.

[4] P. I. Djurovich, E. I. Mayo, S. R. Forrest, and M. E. Thompson, "Measurement of the lowest unoccupied molecular orbital energies of molecular organic semiconductors," *Org. Electron.*, vol. 10, pp. 515–520, 2009.

[5] C. W. Tang, "Two-layer organic photovoltaic cell," *Appl. Phys. Lett.*, vol. 48, pp. 183–185, 1986.

[6] S. Forrest, "The limits to organic photovoltaic cell efficiency," *MRS Bull.,* vol. 30, pp. 28–32, 2005.

[7] P. Peumans, A. Yakimov, and S. R. Forrest, "Small molecular weight organic thin-film photodetectors and solar cells," *J. Appl. Phys.*, vol. 93, pp. 3693–3723, 2003.

[8] P. A. van Hal, R. A. J. Janssen, G. Lanzani, G. Cerullo, M. Zavelani-Rossi, and S. D. Silvestri, "Full temporal resolution of the two-step photoinduced energy-electron transfer in a fullerene-oligothiophene-fullerene triad using sub-10 fs pump-probe spectroscopy," *Chem. Phys. Lett.*, vol. 345, pp. 33–38, 2001.

[9] P. Peumans, S. Uchida, and S. Forrest, "Efficient bulk heterojunction photovoltaic cells using small-molecular-weight organic thin films," *Nature,* vol. 425, pp. 158–162, 2003.

[10] S.-B. Rim and P. Peumans, "The effects of optical interference on exciton diffusion length measurements using photocurrent spectroscopy," *J. Appl. Phys.*, vol. 103, pp. 124515-1–124515-5, 2008.

[11] R. R. Lunt, N. C. Giebink, A. A. Belak, J. B. Benziger, and S. R. Forrest, "Exciton diffusion lengths of organic semiconductor thin films measured by spectrally resolved photoluminescence quenching," *J. Appl. Phys.*, vol. 105, pp. 053711-1–053711-7, 2009.

[12] J. J. M. Halls, C. A. Walsh, N. C. Greenham, E. A. Marseglia, R. H. Friend, S. C. Moratti, and A. B. Holmes, "Efficient photodiodes from interpenetrating polymer networks," *Nature*, vol. 376, pp. 498–500, 1995.

[13] G. Yu, J. Gao, J. C. Hummelen, F. Wudl, and A. J. Heeger, "Polymer photovoltaic cells: Enhanced efficiencies via a network of internal donor-acceptor heterojunctions," *Science*, vol. 270, pp. 1789–1791, 1995.

[14] C. Brabec, N. Sariciftci, and J. Hummelen, "Plastic solar cells," *Adv. Funct. Mater.,* vol. 11, pp. 15–26, 2001.

[15] M. A. Green, K. Emery, Y. Hishikawa, and W. Warta, "Solar cell efficiency tables (version 33)," *Prog. Photovoltaics,* vol. 17, pp. 85–94, 2009.

[16] B. Kippelen and J.-L. Bredas, "Organic photovoltaics," *Energy Environ. Sci.,* vol. 2, pp. 251–261, 2009.

[17] G. Dennler, M. C. Scharber, and C. J. Brabec, "Polymer-fullerene bulk-heterojunction solar cells," *Adv. Mater.,* vol. 21, pp. 1323–1338, 2009.

[18] J. van Duren, X. Yang, J. Loos, C. Bulle-Lieuwma, A. Sieval, J. Hummelen, and R. Janssen, "Relating the morphology of poly(p-phenylene vinylene)/methanofullerene blends to solar-cell performance," *Adv. Funct. Mater.,* vol. 14, pp. 425–434, 2004.

[19] R. A. Marsh, C. Groves, and N. C. Greenham, "A microscopic model for the behavior of nanostructured organic photovoltaic devices," *J. Appl. Phys.*, vol. 101, pp. 083509-1–083509-7, 2007.

[20] J. Rostalski and D. Meissner, "Monochromatic versus solar efficiencies of organic solar cells," *Sol. Energy Mater. Sol. Cell.*, vol. 61, pp. 87–95, 2000.

[21] B. Maennig, J. Drechsel, D. Gebeyehu, P. Simon, F. Kozlowski, A. Werner, F. Li, S. Grundmann, S. Sonntag, M. Koch, K. Leo, M. Pfeiffer, H. Hoppe, D. Meissner, N. Sariciftci, I. Riedel, V. Dyakonov, and J. Parisi, "Organic p-i-n solar cells," *Appl. Phys. A, Mater. Sci. Process.,* vol. 79, pp. 1–14, 2004.

[22] J. Xue, B. Rand, S. Uchida, and S. Forrest, "A hybrid planar-mixed molecular heterojunction photovoltaic cell," *Adv. Mater.,* vol. 17, pp. 66–71, 2005.

[23] P. Sullivan, S. Heutz, S. M. Schultes, and T. S. Jones, "Influence of codeposition on the performance of CuPc-C_{60} heterojunction photovoltaic devices," *Appl. Phys. Lett.*, vol. 84, pp. 1210–1212, 2004.

[24] S. Heutz, P. Sullivan, B. M. Sanderson, S. M. Schultes, and T. S. Jones, "Influence of molecular architecture and intermixing on the photovoltaic, morphological and spectroscopic properties of CuPc-C_{60} heterojunctions," *Sol. Energy Mater. Sol. Cell.*, vol. 83, pp. 229–245, 2004.

[25] F. Yang, M. Shtein, and S. R. Forrest, "Morphology control and material mixing by high-temperature organic vapor-phase deposition and its application to thin-film solar cells," *J. Appl. Phys.*, vol. 98, pp. 014906-1–014906-10, 2005.

[26] C. Mueller, T. A. M. Ferenczi, M. Campoy-Quiles, J. M. Frost, D. D. C. Bradley, P. Smith, N. Stingelin-Stutzmann, and J. Nelson, "Binary organic photovoltaic blends: A simple rationale for optimum compositions," *Adv. Mater.,* vol. 20, pp. 3510–3515, 2008.

[27] O. V. Molodtsova and M. Knupfer, "Electronic properties of the organic semiconductor interfaces CuPc/C_{60} and C_{60}/CuPc," *J. Appl. Phys.*, vol. 99, pp. 053704-1–053704-7, 2006.

[28] S. Krause, M. B. Casu, A. Schöll, and E. Umbach, "Determination of transport levels of organic semiconductors by UPS and IPS," *New J. Phys.*, vol. 10, pp. 085001-1–085001-7, 2008.

[29] M. L. Tang, A. D. Reichardt, P. Wei, and Z. Bao, "Correlating carrier type with frontier molecular orbital energy levels in organic thin film transistors of functionalized acene derivatives," *J. Amer. Chem. Soc.,* vol. 131, pp. 5264–5273, 2009.

[30] N. Koch, A. C. Dürr, J. Ghijsen, R. L. Johnson, J. J. Pireaux, J. Schwartz, F. Schreiber, H. Dosch, and A. Kahn, "Optically induced electron transfer from conjugated organic molecules to charged metal clusters," *Thin Solid Films*, vol. 441, pp. 145–149, 2003.

[31] U. Heinemeyer, R. Scholz, L. Gisslén, M. I. Alonso, J. O. Ossó, M. Garriga, A. Hinderhofer, M. Kytka, S. Kowarik, A. Gerlach, and F. Schreiber, "Exciton-phonon coupling in diindenoperylene thin films," *Phys. Rev. B*, vol. 78, pp. 085210-1–085210-10, 2008.

[32] A. Hinderhofer, U. Heinemeyer, A. Gerlach, S. Kowarik, R. M. J. Jacobs, Y. Sakamoto, T. Suzuki, and F. Schreiber, "Optical properties of pentacene and perfluoropentacene thin films," *J. Chem. Phys.*, vol. 127, pp. 194705-1–194705-6, 2007.

[33] A. Opitz, J. Wagner, M. Bronner, W. Brütting, A. Hinderhofer, and F. Schreiber, "Molecular semiconductor blends: Microstructure, charge carrier transport and application in photovoltaic cells," *Phys. Stat. Sol. (a)*, vol. 206, pp. 2683–2694, 2009.

[34] I. Salzmann, S. Duhm, R. Opitz, R. L. Johnson, J. P. Rabe, and N. Koch, "Structural and electronic properties of pentacene-fullerene heterojunctions," *J. Appl. Phys.*, vol. 104, pp. 114518-1–114518-11, 2008.

[35] V. Shrotriya, G. Li, Y. Yao, T. Moriarty, K. Emery, and Y. Yang, "Accurate measurement and characterization of organic solar cells," *Adv. Funct. Mater.,* vol. 16, pp. 2016–2023, 2006.

[36] T. Stübinger and W. Brütting, "Exciton diffusion and optical interference in organic donor-acceptor photovoltaic cells," *J. Appl. Phys.*, vol. 90, pp. 3632–3641, 2001.

[37] B. Kraabel, D. McBranch, N. S. Sariciftci, D. Moses, and A. J. Heeger, "Ultrafast spectroscopic studies of photoinduced electron-transfer from semiconducting polymers to C_{60}," *Phys. Rev. B*, vol. 50, pp. 18 543–18 552, 1994.

[38] B. P. Rand, J. G. Xue, S. Uchida, and S. R. Forrest, "Mixed donor-acceptor molecular heterojunctions for photovoltaic applications. I. Material properties," *J. Appl. Phys.*, vol. 98, pp. 124902-1–124902-7, 2005.

[39] A. Opitz, M. Bronner, and W. Brütting, "Ambipolar charge carrier transport in mixed organic layers of phthalocyanine and fullerene," *J. Appl. Phys.*, vol. 101, pp. 063709-1–063709-9, 2007.

[40] M. A. Loi, C. Rost-Bietsch, M. Murgia, S. Karg, W. Rieß, and M. Muccini, "Tuning optoelectronic properties of ambipolar organic light-emitting transistors using a bulk-heterojunction approach," *Adv. Funct. Mater.*, vol. 16, pp. 41–47, 2006.

[41] M. Bronner, A. Opitz, and W. Brütting, "Ambipolar charge carrier transport in organic semiconductor blends of phthalocyanine and fullerene," *Phys. Stat. Sol. (a)*, vol. 205, pp. 549–563, 2008.

[42] A. Opitz, M. Bronner, J. Wagner, M. Götzenbrugger, and W. Brütting, "Ambipolar organic semiconductor blends for photovoltaic cells," *Proc. SPIE*, vol. 7002, pp. 70020J-1–70020J-9, 2008.
[43] A. Opitz, M. Bronner, W. Brütting, M. Himmerlich, J. A. Schaefer, and S. Krischok, "Electronic properties of organic semiconductor blends: Ambipolar mixtures of phthalocyanine and fullerene," *Appl. Phys. Lett.*, vol. 90, pp. 212112-1–212112-3, 2007.
[44] C. Uhrich, D. Wynands, S. Olthof, M. K. Riede, K. Leo, S. Sonntag, B. Maennig, and M. Pfeiffer, "Origin of open circuit voltage in planar and bulk heterojunction organic thin-film photovoltaics depending on doped transport layers," *J. Appl. Phys.*, vol. 104, pp. 043107-1–043107-6, 2008.
[45] D. Wynands, B. Männig, M. Riede, K. Leo, E. Brier, E. Reinold, and P. Bäuerle, "Organic thin film photovoltaic cells based on planar and mixed heterojunctions between fullerene and a low bandgap oligothiophene," *J. Appl. Phys.*, vol. 106, pp. 054509-1–054509-5, 2009.
[46] J. Nelson, J. Kirkpatrick, and P. Ravirajan, "Factors limiting the efficiency of molecular photovoltaic devices," *Phys. Rev. B*, vol. 69, pp. 035337-1–035337-11, 2004.
[47] P. Sullivan and T. Jones, "Pentacene/fullerene (C_{60}) heterojunction solar cells: Device performance and degradation mechanisms," *Org. Electron.*, vol. 9, pp. 656–660, 2008.
[48] A. Kumar, S. Sista, and Y. Yang, "Dipole induced anomalous S-shape I-V curves in polymer solar cells," *J. Appl. Phys.*, vol. 105, pp. 094512-1–094512-6, 2009.
[49] M. Glatthaar, M. Riede, N. Keegan, K. Sylvester-Hvida, B. Zimmermann, M. Niggemann, A. Hinsch, and A. Gombert, "Efficiency limiting factors of organic bulk heterojunction solar cells identified by electrical impedance spectroscopy," *Sol. Ener. Mater. Sol. Cell.*, vol. 91, pp. 390–393, 2007.
[50] P. Peumans and S. R. Forrest, "Very-high-efficiency double-heterostructure copper phthalocyanine/C_{60} photovoltaic cells," *Appl. Phys. Lett.*, vol. 79, pp. 126–128, 2001.
[51] P. Peumans, V. Bulović, and S. R. Forrest, "Efficient photon harvesting at high optical intensities in ultrathin organic double-heterostructure photovoltaic diodes," *Appl. Phys. Lett.*, vol. 76, pp. 2650–2652, 2000.
[52] N. Li, B. E. Lassiter, R. R. Lunt, G. Wei, and S. R. Forrest, "Open circuit voltage enhancement due to reduced dark current in small molecule photovoltaic cells," *Appl. Phys. Lett.*, vol. 94, pp. 023307-1–023307-3, 2009.
[53] H. Gommans, B. Verreet, B. P. Rand, R. Muller, J. Poortmans, P. Heremans, and J. Genoe, "On the role of bathocuproine in organic photovoltaic cells," *Adv. Funct. Mater.*, vol. 18, pp. 3686–3691, 2008.
[54] J. Meiss, M. K. Riede, and K. Leo, "Optimizing the morphology of metal multilayer films for indium tin oxide ITO-free inverted organic solar cells," *J. Appl. Phys.*, vol. 105, pp. 063108-1–063108-5, 2009.
[55] M. Knupfer and H. Peisert, "Electronic properties of interfaces between model organic semiconductors and metals," *Phys. Stat. Sol. (a)*, vol. 201, pp. 1055–1074, 2004.
[56] H. Brinkmann, C. Kelting, S. Makarov, O. Tsaryova, G. Schnurpfeil, D. Wöhrle, and D. Schlettwein, "Fluorinated phthalocyanines as molecular semiconductor thin films," *Phys. Stat. Sol. (a),* vol. 205, pp. 409–420, 2008.
[57] A. Opitz, B. Ecker, J. Wagner, A. Hinderhofer, F. Schreiber, J. Manara, J. Pflaum, and W. Brütting, "Mixed crystalline films of co-evaporated hydrogen- and fluorine-terminated phthalocyanines and their application in photovoltaic devices," *Org. Electron.*, vol. 10, pp. 1259–1267, 2009.
[58] I. Salzmann, S. Duhm, G. Heimel, J. P. Rabe, N. Koch, M. Oehzelt, Y. Sakamoto, and T. Suzuki, "Structural order in perfluoropentacene thin films and heterostructures with pentacene," *Langmuir*, vol. 24, pp. 7294–7298, 2008.
[59] J.-O. Vogel, I. Salzmann, R. Opitz, S. Duhm, B. Nickel, J. P. Rabe, and N. Koch, "Sub-nanometer control of the interlayer spacing in thin films of intercalated rodlike conjugated molecules," *J. Phys. Chem. B*, vol. 111, pp. 14 097–14 101, 2007.
[60] M. Kröger, S. Hamwi, J. Meyer, T. Dobbertin, T. Riedl, W. Kowalsky, and H.-H. Johannes, "Temperature-independent field-induced charge separation at doped organic/organic interfaces: Experimental modeling of electrical properties," *Phys. Rev. B,* vol. 75, pp. 235321-1–235321-8, 2007.
[61] A. Facchetti, "Semiconductors for organic transistors," *Mater. Today*, vol. 10, pp. 28–37, 2007.
[62] S. Yoo, B. Domercq, and B. Kippelen, "Efficient thin-film organic solar cells based on pentacene/C_{60} heterojunctions," *Appl. Phys. Lett.*, vol. 85, pp. 5427–5429, 2004.
[63] A. K. Pandey and J.-M. Nunzi, "Efficient flexible and thermally stable pentacene/C_{60} small molecule based organic solar cells," *Appl. Phys. Lett.*, vol. 89, pp. 213506-1–213506-3, 2006.
[64] A. C. Dürr, F. Schreiber, M. Münch, N. Karl, B. Krause, V. Kruppa, and H. Dosch, "High structural order in thin films of the organic semiconductor diindenoperylene," *Appl. Phys. Lett.*, vol. 81, pp. 2276–2278, 2002.
[65] R. Resel, N. Koch, F. Meghdadi, G. Leising, W. Unzog, and K. Reichmann, "Growth and preferred crystallographic orientation of hexaphenyl thin films," *Thin Solid Films*, vol. 305, pp. 232–242, 1997.
[66] B. Servet, S. Ries, M. Trotel, P. Alnot, G. Horowitz, and F. Garnier, "X-ray determination of the crystal structure and orientation of vacuum evaporated sexithiophene films," *Adv. Mater.*, vol. 5, pp. 461–464, 1993.
[67] D. Fujishima, H. Kanno, T. Kinoshita, E. Maruyama, M. Tanaka, M. Shirakawa, and K. Shibata, "Organic thin-film solar cell employing a novel electron-donor material," *Sol. Ener. Mater. Sol. Cell.*, vol. 93, pp. 1029–1032, 2009.
[68] A. K. Tripathi and J. Pflaum, "Correlation between ambipolar transport and structural phase transition in diindenoperylene single crystals," *Appl. Phys. Lett.*, vol. 89, pp. 082103-1–082103-3, 2006.
[69] D. Kurrle and J. Pflaum, "Exciton diffusion length in the organic semiconductor diindenoperylene," *Appl. Phys. Lett.*, vol. 92, pp. 133306-1–133306-3, 2008.
[70] R. R. Lunt, J. B. Benziger, and S. R. Forrest, "Relationship between crystalline order and exciton diffusion length in molecular organic semiconductors," *Adv. Mater.*, vol. 22, pp. 1233–1236, 2010.
[71] J. Wagner, M. Gruber, A. Wilke, A. Hinderhofer, A. Vollmer, A. Opitz, N. Koch, F. Schreiber, and W. Brütting, "High fill factor and open circuit voltage in organic photovoltaic cells with diindenoperylene as donor material," submitted for publication.
[72] B. P. Rand, D. P. Burk, and S. R. Forrest, "Offset energies at organic semiconductor heterojunctions and their influence on the open-circuit voltage of thin-film solar cells," *Phys. Rev. B*, vol. 75, pp. 115327-1–115327-11, 2007.
[73] S. Veenstra, G. Malliaras, H. Brouwer, F. Esselink, V. Krasnikov, P. van Hutten, J. Wildeman, H. Jonkman, G. Sawatzky, and G. Hadziioannou, "Sexithiophene-C_{60} blends as model systems for photovoltaic devices," *Synthetic Met.*, vol. 84, pp. 971–972, 1997.
[74] S. Alem, A. K. Pandey, K. N. N. Unni, J.-M. Nunzi, and P. Blanchard, "Molecular model T6:C_{60} bulk-heterojunction solar cells," *J. Vac. Sci. Technol. A*, vol. 24, pp. 645–648, 2006.
[75] J. Zhang, I. Salzmann, S. Rogaschewski, J. P. Rabe, N. Koch, F. Zhang, and Z. Xu, "Arrays of crystalline C_{60} and pentacene nanocolumns," *Appl. Phys. Lett.*, vol. 90, pp. 193117-1–193117-3, 2007.
[76] M.-S. Kim, J.-S. Kim, J. C. Cho, M. Shtein, L. J. Guo, and J. Kim, "Flexible conjugated polymer photovoltaic cells with controlled heterojunctions fabricated using nanoimprint lithography," *Appl. Phys. Lett.*, vol. 90, pp. 123113-1–123113-3, 2007.
[77] D. Cheyns, K. Vasseur, C. Rolin, J. Genoe, J. Poortmans, and P. Heremans, "Nanoimprinted semiconducting polymer films with 50 nm features and their application to organic heterojunction solar cells," *Nanotechnology*, vol. 19, pp. 424016-1–424016-6, 2008.

Andreas Opitz received the Ph.D. degree in physics from the Technical University of Ilmenau, Ilmenau, Germany, in 2003.

He joined the University of Augsburg, Augsburg, Germany, where he is involved in charge-carrier transport in organic semiconductors focused on field-effect transistors and photovoltaic cells using molecular and polymeric materials, and has been a Lecturer of experimental physics, since 2009. His current research include charge transport, injection and separation properties at organic/organic and organic/inorganic interfaces.

Julia Wagner received the M.Sc. degree in material science from the University of Augsburg, Augsburg, Germany. Since 2008, she has been working toward the Ph.D. degree in the group of Prof. W. Brütting.

Her research interests include charge transport and device performance of organic solar cells based on small molecules.

Wolfgang Brütting received the Ph.D. degree in physics from the University of Bayreuth, Bayreuth, Germany, in 1995 with a study on charge transport in 1-D charge-density wave systems.

He then moved to the field of organic semiconductors, where he was involved in the development of organic light-emitting devices for display applications. Since 2003, he has been a Professor of experimental physics at the University of Augsburg, Augsburg, Germany. His research interests include physics of organic semiconductors, including thin film growth, photophysics and electrical transport of these materials, and related electronic devices.

Ingo Salzmann received the Diploma degree in physics from the Graz University of Technology, Graz, Austria, and the Ph.D. degree from the Humboldt-Universität zu Berlin, Berlin, Germany, in 2008, in the groups of J. P. Rabe and N. Koch.

He is currently a Postdoctoral Research Associate at the Humboldt-Universität zu Berlin. His research interests include structure–energetic correlations in thin organic films regarding applications in organic electronics, mainly using X-ray scattering techniques and photoelectron spectroscopy as experimental tools.

Norbert Koch received the Ph.D. degree in physics from the Graz University of Technology, Graz, Austria, in 2000.

He was a Postdoctoral Researcher at Princeton University, Princeton, NJ, until 2002. He was a Research Associate in the group of J. P. Rabe at the Humboldt-Universität zu Berlin, Germany and was the Head of a junior research group in the Emmy Noether Program (DFG) from 2004–2009. Since 2009, he has been a Full Professor at Humboldt-Universität, Berlin. His research interests include electronic and structural properties of complex functional interfaces with organic materials, and the exploration of new strategies for organic–organic and organic–inorganic heterostructure fabrication.

Jochen Manara received the Ph.D. degree in physics from Julius Maximilian University, Würzburg, Germany, in 2001.

In 2002, he became the Manager of the Applied IR Metrology group at ZAE Bayern, Würzburg. His current research interests include optical and infrared-optical characterization of solids and thin films, which involves the analytical and numerical modeling of radiative transfer through materials and between surfaces.

Jens Pflaum received the Ph.D. degree from Bochum University, Bochum, Germany, in 1999.

He was a Postdoctoral Research Fellow at Princeton University. During 2001–2008, he was involved in research on transport phenomena in organic crystals at Stuttgart University. In 2008, he became a Professor at Würzburg University and the Group Leader of the Organic Photovoltaics and Electronics Division, ZAE Bayern, where he is involved in molecular optoelectronics. He is an expert for molecular solid-state physics.

Alexander Hinderhofer received the M.Sc. (diploma) degree in physics from Eberhard Karls University, Tübingen, Germany. Since 2007 he has been working toward the Ph.D. degree at the Institute of Applied Physics, University of Tübingen, Tübingen, in the group of Prof. Schreiber.

His current research interests include optical and structural characterization of organic heterostructure interfaces in real time during growth.

Frank Schreiber received the Ph.D. degree from Bochum University, Bochum, Germany, in 1995.

He was a Postdoctoral Research Fellow at Princeton University. He joined the Max Planck institute and university, Stuttgart, in 1997, where he to led the organic thin films group. During 2002–2004, he was a University Lecturer in Oxford University, U.K. He is currently a Full Professor at the University of Tübingen, Tübingen, Germany, and is involved in the physics of molecular and biological matter.